

# Astrocyte reactivity influences amyloid- $\beta$ effects on tau pathology in preclinical Alzheimer's disease

Received: 23 January 2023

Accepted: 1 May 2023

Published online: 29 May 2023

 Check for updates

Bruna Bellaver <sup>1,2</sup>, Guilherme Povala <sup>1</sup>, Pamela C. L. Ferreira <sup>1</sup>, João Pedro Ferrari-Souza<sup>1,2</sup>, Douglas T. Leffa<sup>1</sup>, Firoza Z. Lussier<sup>1</sup>, Andréa L. Benedet<sup>3</sup>, Nicholas J. Ashton<sup>3,4,5</sup>, Gallen Triana-Baltzer<sup>6</sup>, Hartmuth C. Kolb<sup>6</sup>, Cécile Tissot <sup>7</sup>, Joseph Therriault <sup>7</sup>, Stijn Servaes<sup>7</sup>, Jenna Stevenson<sup>7</sup>, Nesrine Rahmouni<sup>7</sup>, Oscar L. Lopez <sup>8</sup>, Dana L. Tudorascu<sup>1,9</sup>, Victor L. Villemagne<sup>1</sup>, Milos D. Ikonomovic<sup>1,8,10</sup>, Serge Gauthier<sup>7</sup>, Eduardo R. Zimmer<sup>2,11,12,13</sup>, Henrik Zetterberg <sup>3,14,15,16,17,18</sup>, Kaj Blennow <sup>3,14</sup>, Howard J. Aizenstein<sup>1,19</sup>, William E. Klunk<sup>1</sup>, Beth E. Snitz<sup>8</sup>, Pauline Maki<sup>20</sup>, Rebecca C. Thurston <sup>1,21,22</sup>, Ann D. Cohen<sup>1</sup>, Mary Ganguli<sup>1,8,22</sup>, Thomas K. Karikari<sup>1,3</sup>, Pedro Rosa-Neto <sup>7,23</sup> & Tharick A. Pascoal <sup>1,8</sup> ✉

An unresolved question for the understanding of Alzheimer's disease (AD) pathophysiology is why a significant percentage of amyloid- $\beta$  (A $\beta$ )-positive cognitively unimpaired (CU) individuals do not develop detectable downstream tau pathology and, consequently, clinical deterioration. In vitro evidence suggests that reactive astrocytes unleash A $\beta$  effects in pathological tau phosphorylation. Here, in a biomarker study across three cohorts ( $n = 1,016$ ), we tested whether astrocyte reactivity modulates the association of A $\beta$  with tau phosphorylation in CU individuals. We found that A $\beta$  was associated with increased plasma phosphorylated tau only in individuals positive for astrocyte reactivity (Ast<sup>+</sup>). Cross-sectional and longitudinal tau-positron emission tomography analyses revealed an AD-like pattern of tau tangle accumulation as a function of A $\beta$  only in CU Ast<sup>+</sup> individuals. Our findings suggest astrocyte reactivity as an important upstream event linking A $\beta$  with initial tau pathology, which may have implications for the biological definition of preclinical AD and for selecting CU individuals for clinical trials.

Rapid advances in fluid and neuroimaging biomarkers have facilitated the understanding of the dynamic associations between Alzheimer's disease (AD)-related pathophysiological processes in the living human brain. These biomarker studies suggest that brain accumulation of amyloid- $\beta$  (A $\beta$ ) precedes tau pathology in cognitively unimpaired (CU) individuals<sup>1–3</sup>, which is closely related to the development of cognitive symptoms<sup>4–6</sup>. However, the reasons why A $\beta$  pathology is not associated with AD-related progression in some CU individuals is one of the most pressing questions in the field<sup>7–9</sup>. In addition to revealing key biological

players associated with disease progression, finding predictive markers of early A $\beta$ -related tau pathology would allow for the identification of CU individuals who are more likely to develop AD even before the first signs of pathological tau, facilitating enrollment in early prevention clinical trials<sup>10</sup>.

The fact that A $\beta$  leads to tau pathology in some individuals, but not in others, suggests the presence of other biological processes capable of triggering the deleterious effects of A $\beta$  in the early disease stages. Postmortem studies show that astrocyte reactivity is a

**Table 1 | Demographics and key characteristics of participants**

Characteristics	A $\beta^-$ /Ast $^-$ (n=557)	A $\beta^-$ /Ast $^+$ (n=165)	A $\beta^+$ /Ast $^-$ (n=186)	A $\beta^+$ /Ast $^+$ (n=108)
Age, mean (s.d.)	68.2 (8.6)	72.1 (8.2) <sup>a</sup>	68.6 (7.6) <sup>b</sup>	74.7 (10.6) <sup>a,c</sup>
Sex, n (% female)	367 (65.9)	137 (83.0) <sup>a</sup>	122 (65.6) <sup>b</sup>	79 (73.1)
MMSE/MoCA, mean (s.d.)	28.1 (3.3)/27.5 (1.8)	28.1 (3.2)/28.1 (1.7)	27.8 (3.2)/26.7 (4.1) <sup>b</sup>	27.1 (6.1)/27.2 (1.4)
APOE $\epsilon$ 4 (% of carriers)	89 (16.0)	25 (15.2)	33 (17.7)	25 (23.1)
Education, years (s.d.)	15.0 (2.7)	15.2 (3.1)	14.8 (2.7)	15.0 (2.8)
A $\beta$ burden (z score, s.d.)	-0.52 (0.65)	-0.40 (0.57)	1.17 (0.63) <sup>a,b</sup>	1.25 (0.69) <sup>a,b</sup>
Plasma GFAP (z score, s.d.)	-0.50 (0.51)	1.20 (0.75) <sup>a</sup>	-0.42 (0.52) <sup>b</sup>	1.48 (0.88) <sup>a,b,c</sup>
Plasma p-tau181 (z score, s.d.)	-0.12 (0.90)	0.10 (0.82) <sup>a</sup>	-0.14 (0.97)	0.77 (1.89) <sup>a,b,c</sup>
Plasma p-tau231 (z score, s.d.)	-0.03 (1.00)	-0.12 (0.82)	-0.04 (0.86)	0.55 (1.26) <sup>a,b,c</sup>
Plasma p-tau217 (z score, s.d.)	-0.27 (0.38)	-0.24 (0.38)	0.17 (0.49)	1.12 (1.99) <sup>a,b,c</sup>
Plasma neurofilament light (z score, s.d.)	-0.24 (0.62)	0.42 (0.99) <sup>a</sup>	-0.13 (1.22) <sup>b</sup>	0.80 (1.47) <sup>a,b,c</sup>

Missing APOE  $\epsilon$ 4: 140 A $\beta^-$ /Ast $^-$ , 43 A $\beta^-$ /Ast $^+$ , 45 A $\beta^+$ /Ast $^-$  and 17 A $\beta^+$ /Ast $^+$ . Missing neurofilament light: 2 A $\beta^-$ /Ast $^-$ , 2 A $\beta^-$ /Ast $^+$  and 1 A $\beta^+$ /Ast $^-$ . Plasma p-tau231 is available for a subset of participants from TRIAD and Pittsburgh cohorts. Plasma p-tau217 is available for a subset of participants from the TRIAD cohort. <sup>a</sup>Different from A $\beta^-$ /Ast $^-$ . <sup>b</sup>Different from A $\beta^-$ /Ast $^+$ . <sup>c</sup>Different from A $\beta^+$ /Ast $^-$ .

common neuropathological finding in CU individuals and, like cortical A $\beta$  plaques, one of the earliest abnormalities in AD<sup>11–15</sup>. Experimental literature suggests that astrocyte reactivity is critical for triggering A $\beta$ -induced tau phosphorylation<sup>16</sup> and that the attenuation of astrocyte reactivity mitigates tau pathology<sup>17,18</sup>. Additionally, glial fibrillary acidic protein (GFAP)-positive astrocytes can internalize tau and may contribute to its propagation<sup>19,20</sup>. Altogether, these experimental results support a close link between A $\beta$ , astrocyte reactivity and tau.

Clinical studies support that plasma measures of GFAP correlate with its CSF levels and are increased in CU individuals with AD pathophysiology, representing a robust proxy of astrocyte reactivity in the brains of these individuals<sup>21–24</sup>. Based on this previous literature, we designed a multisite biomarker study including three cohorts to test the hypothesis that the presence of astrocyte reactivity biomarker abnormality is a key element in determining the association of A $\beta$  burden with early tau phosphorylation and aggregation biomarkers in preclinical AD.

## Results

### Participants

We investigated 1,016 CU individuals (mean age = 69.6  $\pm$  8.9, clinical dementia rating (CDR) = 0) from two research (Translational Biomarkers in Aging and Dementia (TRIAD), McGill University, Canada and Pittsburgh, University of Pittsburgh, USA) and one population-based (Monongahela-Youghiogheny Healthy Aging Team (MYHAT), Pittsburgh, USA) cohorts with in vivo biomarkers. Individuals were classified as negative (Ast $^-$ ) or positive (Ast $^+$ ) for astrocyte reactivity based on their plasma GFAP levels. Demographic and clinical characteristics of participants are summarized in Table 1. Overall, participants classified as A $\beta^+$ /Ast $^+$  presented increased plasma phosphorylated tau (p-tau)181, p-tau231 and p-tau217 compared to other groups. No differences in A $\beta$  levels were observed between CU A $\beta^+$ /Ast $^-$  and A $\beta^+$ /Ast $^+$  in any cohort. Demographic characteristics of individuals segregated by cohort are presented in Supplementary Tables 1–3.

### Astrocyte reactivity affects A $\beta$ -dependent tau phosphorylation

We z scored biomarker levels inside each cohort and applied a robust linear regression to model the trajectory of plasma p-tau181, the only p-tau biomarker available in all cohorts, as a function of A $\beta$  burden (plasma or positron emission tomography (PET)) in CU individuals classified as Ast $^-$  (n = 743) or Ast $^+$  (n = 273). Notably, we observed that plasma p-tau181 levels increased as a function of A $\beta$  only in CU Ast $^+$  individuals (Fig. 1a). Similarly, linear regression showed a significant association between

A $\beta$  burden and plasma p-tau181 in CU Ast $^+$  ( $\beta$  = 0.34,  $t$  = 5.37,  $P$  < 0.0001; Fig. 1b and Extended Data Table 1) but not in CU Ast $^-$  ( $\beta$  = 0.04,  $t$  = 1.06,  $P$  = 0.29; Fig. 1b) individuals. A significant interaction between A $\beta$  burden and astrocyte reactivity status on plasma p-tau181 ( $\beta$  = 0.31,  $t$  = 4.62,  $P$  < 0.0001; Fig. 1b) further supported that the presence of astrocyte reactivity was key to determining A $\beta$  effects on tau phosphorylation. These results were replicated using different cutoff values to determine reactive astrocyte positivity (Extended Data Table 2). In addition, linear regression using only continuous values for A $\beta$ , p-tau181 and GFAP levels confirmed that these results were not driven by biomarker thresholds ( $\beta$  = 0.10,  $t$  = 3.22,  $P$  = 0.0013; Fig. 1c). Cohen's  $d$  analysis revealed that the presence of both A $\beta^+$  and Ast $^+$  has a large magnitude of effect on tau phosphorylation (Cohen's  $d$  = 0.80), whereas A $\beta^+$  in the absence of Ast $^+$  presented a negligible effect size (Fig. 1d). Voxel-wise analysis confirmed that A $\beta$  levels associated with plasma p-tau181 only in the presence of astrocyte reactivity in some brain regions previously shown to present early A $\beta$  pathology in PET studies, including the posterior cingulate, precuneus and insula<sup>25</sup> (Fig. 1e).

Consistently, the stratified analysis within cohorts showed similar results. In the three enrollment sites, plasma p-tau181 levels increased as a function of A $\beta$  burden only in CU Ast $^+$  (Pittsburgh:  $\beta$  = -0.35,  $t$  = 3.10,  $P$  = 0.003 (Fig. 1f); MYHAT:  $\beta$  = -0.20,  $t$  = 2.26,  $P$  = 0.026 (Fig. 1h) and TRIAD:  $\beta$  = 0.57,  $t$  = 4.36,  $P$  < 0.0001 (Fig. 1j)). A steeper increase in plasma p-tau181 was observed in the research cohorts (TRIAD and Pittsburgh) compared to the population-based cohort (MYHAT). Similarly, we observed a significant interaction between A $\beta$  burden and astrocyte reactivity status on plasma p-tau181 levels in the Pittsburgh ( $\beta$  = -0.29,  $t$  = 2.30,  $P$  = 0.022; Fig. 1g), MYHAT ( $\beta$  = -0.19,  $t$  = 2.07,  $P$  = 0.039; Fig. 1i) and TRIAD ( $\beta$  = 0.46,  $t$  = 2.92,  $P$  = 0.004; Fig. 1k) cohorts. In a subset of participants from the Pittsburgh and MYHAT cohorts with available A $\beta$ -PET (n = 150), we also found increased plasma p-tau181 as a function of A $\beta$ -PET only in Ast $^+$  (Extended Data Fig. 1). No significant effect of apolipoprotein  $\epsilon$ 4 (APOE  $\epsilon$ 4) status was observed in the aforementioned associations (Extended Data Table 3).

We also explored the impact of Ast $^+$  in the associations of A $\beta$  burden with plasma p-tau231 (available for Pittsburgh and TRIAD cohorts, n = 502) and p-tau217 (available for the TRIAD cohort, n = 136) levels in subsets of individuals that had these markers available. Plasma p-tau231 increased as a function of A $\beta$  only in CU Ast $^+$  individuals (Fig. 1l). Additionally, we found a significant association between A $\beta$  and plasma p-tau231 in CU Ast $^+$  ( $\beta$  = 0.36,  $t$  = 4.62,  $P$  < 0.0001; Fig. 1m and Extended Data Table 3) but not in CU Ast $^-$  individuals ( $\beta$  = 0.10,  $t$  = 1.87,  $P$  = 0.06). We also observed a significant interaction between A $\beta$  and astrocyte reactivity status on plasma p-tau231 ( $\beta$  = 0.26,  $t$  = 2.84,  $P$  = 0.004; Fig. 1m).

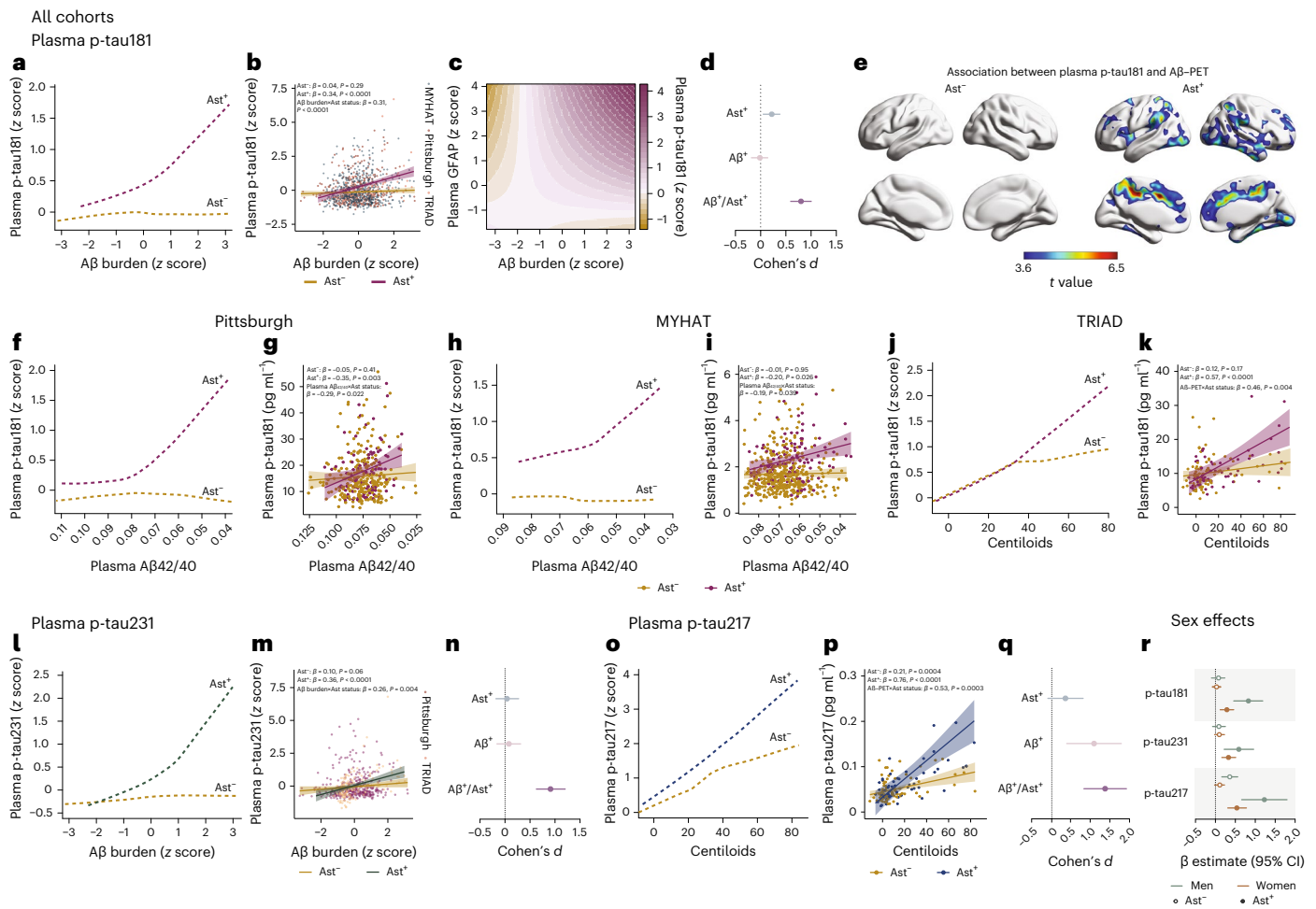


**Fig. 1 | Astrocyte reactivity influences Aβ-dependent tau phosphorylation.**

**a**, Robust linear regressions show that plasma p-tau181 increases as a function of Aβ burden only in the presence of astrocyte reactivity (Ast<sup>+</sup>) in all cohorts together ( $n = 1,016$ ). **b**, Linear regressions adjusted for age and sex revealed an interaction between Aβ burden and astrocyte reactivity status on p-tau181 levels in all cohorts ( $n = 1,016$ ). Shaded areas represent 95% confidence intervals of the regression lines. **c**, Continuous association between Aβ pathology, plasma p-tau181 and plasma GFAP adjusted for age and sex ( $n = 1,016$ ). **d**, Cohen's *d* analysis accounting for age and sex shows the effect sizes of Aβ and astrocyte reactivity status on plasma p-tau181 ( $n = 1,016$ ). The error bars represent the 95% confidence interval. **e**, Voxel-wise regressions, corrected for multiple comparisons, show that Aβ-PET is associated with plasma p-tau181 only in CU Ast<sup>+</sup> in typical AD regions (TRIAD cohort,  $n = 147$ ). **f–k**, Robust locally weighted and linear regressions adjusted for age and sex show that plasma p-tau181 increases as a function of Aβ burden only in Ast<sup>+</sup> individuals and with a significant interaction between Aβ and astrocyte reactivity status on p-tau181 levels in (**f,g**) Pittsburgh ( $n = 355$ ), (**h,i**) MYHAT ( $n = 514$ ) and (**j,k**) TRIAD ( $n = 147$ ) cohorts. Shaded areas represent 95% confidence intervals of the regression lines. **l,m**, Robust locally weighted and linear regressions adjusted for age and sex

show that (**l**) plasma p-tau231 increases as a function of Aβ burden only in Ast<sup>+</sup> individuals and with (**m**) a significant interaction between Aβ burden and astrocyte reactivity status on p-tau231 ( $n = 502$ ). **n**, Cohen's *d* analysis accounting for age and sex shows the effect sizes of Aβ and astrocyte reactivity status on plasma p-tau231 ( $n = 502$ ). The error bars represent the 95% confidence intervals. **o,p**, Robust locally weighted and linear regressions adjusted for age and sex show that (**o**) plasma p-tau217 increases as a function of Aβ burden only in Ast<sup>+</sup> individuals and with (**p**) a significant interaction between Aβ burden and astrocyte reactivity status on p-tau217 ( $n = 136$ ). Shaded areas represent 95% confidence intervals of the regression lines. For illustrative purposes only, two individuals with high plasma p-tau181 and p-tau217 concentrations were not shown in **k** and **p**, but they were fully included in the statistical analyses. **q**, Cohen's *d* analysis accounting for age and sex shows the effect sizes of Aβ and astrocyte reactivity status on plasma p-tau217 ( $n = 136$ ). The error bars represent the 95% confidence intervals. **r**, β estimates with respective 95% confidence interval of linear regressions showing the effect of sex on the associations of Aβ with plasma p-tau epitopes in Ast<sup>-</sup> and Ast<sup>+</sup> ( $n = 1,016$ ). Green dots represent men and orange dots women. Solid dots represent Ast<sup>+</sup> individuals.

Cohen's *d* analysis suggests that the presence of both Aβ<sup>+</sup> and Ast<sup>+</sup> also had a strong effect on the levels of plasma p-tau231 (Cohen's *d* = 0.91), whereas pathologies independently did not have a significant effect (Fig. 1n). Similarly, plasma p-tau217 presented a steeper increase as a function of Aβ burden in Ast<sup>+</sup> compared to Ast<sup>-</sup> (Fig. 1o and Extended Data Table 4). An association between Aβ burden and plasma p-tau217 was observed in Ast<sup>-</sup> ( $\beta = 0.21, t = 3.74, P = 0.0004$ ; Fig. 1p), but with a much larger magnitude in Ast<sup>+</sup> ( $\beta = 0.76, t = 5.91, P < 0.0001$ ; Fig. 1p). The stronger association in CU Ast<sup>+</sup> individuals was further evidenced by a significant interaction between Aβ burden and astrocyte reactivity

status on plasma p-tau217 ( $\beta = 0.53, t = 3.74, P = 0.0003$ ; Fig. 1p). The presence of both Aβ<sup>+</sup> and Ast<sup>+</sup> had the largest effect size on plasma p-tau217 increase (Cohen's *d* = 1.41; Fig. 1q) compared to p-tau181 and p-tau231. Notably, the presence of astrocyte reactivity did not impact the association between Aβ burden and neurofilament light levels in any of the three cohorts (Supplementary Table 4), supporting that astrocyte reactivity unleashes Aβ effects on early tau pathology but not on neurodegeneration. We did not observe a significant effect of microglial activation abnormality on the association between Aβ and p-tau in a subset of individuals with available CSF soluble triggering

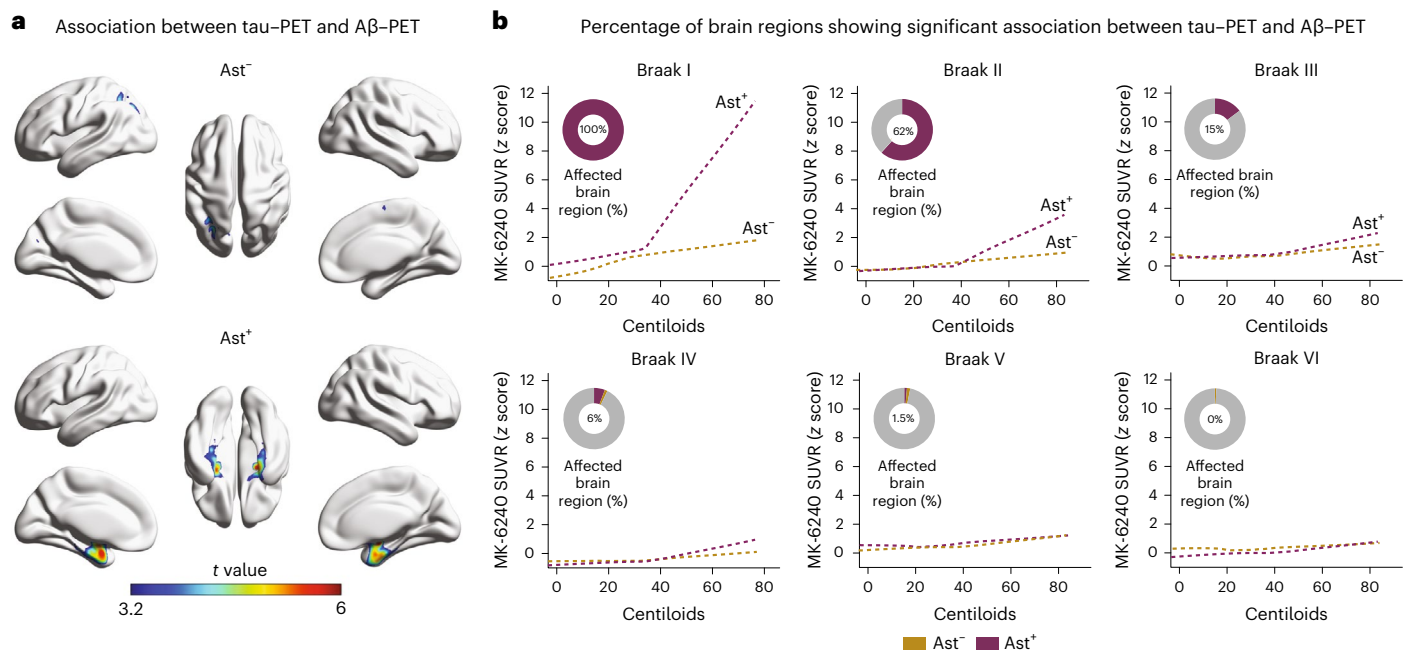


**Fig. 2 | Astrocyte reactivity impacts the association of Aβ with tau-PET deposition.** **a**, Voxel-wise regression analysis showing the association between Aβ-PET and tau-PET in individuals classified as negative (Ast<sup>-</sup>) or positive (Ast<sup>+</sup>) for astrocyte reactivity ( $n = 147$ ). **b**, Percentage of the extent of the brain region

with significant association (after RFT correction) between tau-PET and Aβ-PET in each Braak region. Associations were tested using voxel-wise linear regression models corrected for RFT multiple comparison and adjusted by age and sex. RFT, random field theory.

receptor expressed on myeloid cells 2 (sTREM2) in the TRIAD cohort, whereas the effect of astrocyte reactivity remained present in this subgroup ( $n = 67$ ; Extended Data Table 5).

### Sex affects the association of astrocyte reactivity, Aβ and tau

We further investigated whether the effects of astrocyte reactivity on the association between Aβ and p-tau differ between men and women. In Ast<sup>+</sup>, men presented a higher magnitude of association between Aβ and plasma p-tau181 (men  $-\beta = 0.72$ ,  $P < 0.0001$ ; women  $-\beta = 0.27$ ,  $P = 0.00011$ ; Fig. 1r; Extended Data Fig. 2 and Supplementary Fig. 1), p-tau231 (men  $-\beta = 0.59$ ,  $P = 0.0013$ ; women  $-\beta = 0.33$ ,  $P = 0.0003$ ; Fig. 1r and Extended Data Fig. 2) and p-tau217 (men  $-\beta = 1.23$ ,  $P = 0.0009$ ; women  $-\beta = 0.54$ ,  $P < 0.0001$ ; Fig. 1r and Extended Data Fig. 2) compared to women. A significant interaction between Aβ and sex on plasma p-tau181 ( $\beta = 0.47$ ,  $P = 0.005$ ; Extended Data Fig. 2) and p-tau217 ( $\beta = 1.01$ ,  $P = 0.002$ ; Extended Data Fig. 2), but not p-tau231 ( $\beta = 0.26$ ,  $P = 0.27$ ; Extended Data Fig. 2), was observed in the Ast<sup>+</sup> group.

### Astrocyte reactivity impacts Aβ and tau tangle association

We used tau-PET imaging available in the TRIAD cohort to determine the topographic localization of p-tau protein aggregates in the form of tangles ( $n = 147$ ). Tau-PET deposition occurred as a function of Aβ-PET only in CU Ast<sup>+</sup> and in regions expected to present the earliest tau deposition (Fig. 2a), affecting 100% and 62% of the extension of the Braak I and II regions, respectively (Fig. 2b). As expected, in later Braak regions tau-PET, uptake did not increase as a function of Aβ in either group (Fig. 2b).

### Astrocyte reactivity affects longitudinal tau tangle accumulation

We investigated the link of baseline Aβ and astrocyte reactivity status with future tau-PET burden ( $n = 71$ ; mean follow-up = 2.3 years; Supplementary Table 5). We observed that the annual rate of tau-PET accumulation was higher in CU Ast<sup>+</sup> (Fig. 3a) and was predicted by baseline Aβ burden only in CU Ast<sup>+</sup> (Fig. 3b). Interestingly, while the baseline

association was confined to the mesial temporal cortex, the longitudinal tau-PET accumulation as a function of Aβ/Ast presented initial tau spread over the neocortex in Braak III-IV regions (32.5% of Braak III and 30% of Braak IV areas; Fig. 3c), further supporting the notion that these individuals are following a tau accumulation pathway consistent with AD progression<sup>26</sup>.

## Discussion

In summary, we provide biomarker evidence across multiple cohorts that shows that increased astrocyte reactivity, as indicated by elevated plasma GFAP, plays a role in the association of Aβ with early tau phosphorylation in preclinical AD.

The fact that the presence of abnormal astrocyte reactivity determined Aβ-triggered tau pathology in CU individuals may prove to favor the inclusion of astrocyte reactivity biomarkers in the biomarker modeling<sup>1</sup> and biological definitions<sup>27</sup> of AD. Our findings support previous biomarker studies in suggesting that plasma p-tau levels rise in response to early Aβ in preclinical AD<sup>3</sup> but also add that this occurs mainly in the concomitant presence of astrocyte reactivity biomarker abnormality. These results suggest that astrocyte reactivity abnormality could be placed as an early upstream event, likely before tau pathology, in the hypothetical biomarker models of AD progression<sup>28</sup>. Furthermore, we can argue that an Aβ/Ast/p-tau biomarker scheme could provide a more granular early classification for preclinical AD. Specifically, CU classified as Ast<sup>+</sup> and Ast<sup>-</sup> would be more likely to progress to tau positivity, which is closely related to the development of neurodegeneration and cognitive decline<sup>6,29,30</sup>. Further studies measuring Aβ, tau and GFAP biomarkers at multiple time points with long follow-up durations are needed to confirm the temporal order of appearance of each biomarker abnormality and to determine other possible factors associated with early astrocyte reactivity in preclinical AD.

Our results may have implications for clinical trials. As clinical trials have increasingly focused on individuals in the earliest preclinical phases of AD, our results highlight that the selection of Aβ<sup>+</sup>/Ast<sup>+</sup> CU

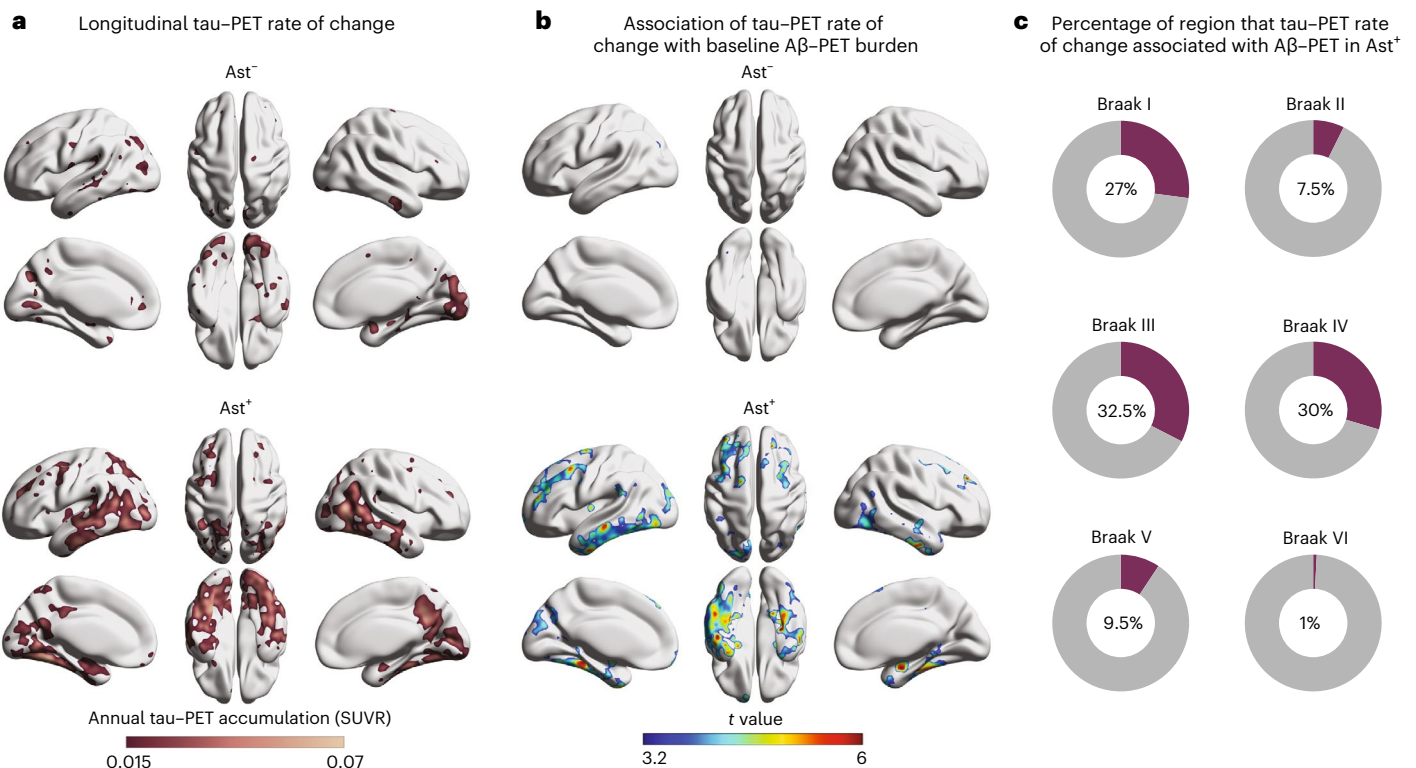


**Fig. 3 | Astrocyte reactivity potentiates longitudinal tau tangle accumulation.** **a**, Longitudinal tau-PET annual rate of change according to astrocyte reactivity status ( $n = 71$ ). **b**, Association between tau-PET annual rate of change and baseline Aβ-PET according to astrocyte reactivity status.

**c**, Percentage of voxels with significant association (after RFT correction) between tau-PET annual rate of change and baseline Aβ-PET in each Braak region. Associations were tested using voxel-wise linear regression models corrected for RFT multiple comparison and adjusted by age and sex.

individuals without overt p-tau abnormality may offer a time window very early in the disease process but with an increased risk of AD-related progression. Although our sensitivity analysis supported plasma GFAP levels 2 s.d. above the mean of CU devoid of detectable Aβ as a robust cutoff to enhance Aβ and p-tau association, a cutoff validation using antemortem blood samples associated with postmortem GFAP characterization is desirable. In addition, experimental literature suggests as a possible mechanism underlying our findings that Aβ-mediated astrocyte signaling (for example, through cytokines, caspases and reactive oxygen species) induces tau pathology<sup>3,13,29</sup>, which is corroborated by studies showing that the suppression of this signaling is able to halt tau phosphorylation<sup>17</sup>. Thus, we can speculate that a combination of drugs targeting Aβ and reactive astrocyte mediators may potentiate the prevention of early tau pathology in trials conducted in preclinical AD individuals.

We found that the effect of astrocyte reactivity on the association between Aβ and tau phosphorylation was greater in CU men than women. Previous studies have shown increased tau biomarkers in women compared to men; however, whether this is driven by Aβ or other sex-specific factors remains unclear<sup>31–33</sup>. Therefore, our results showing that astrocyte reactivity had a greater impact on the association of Aβ with tau in men does not contradict the above-mentioned previous studies. In fact, our findings might be reflected in the recent outcomes of anti-Aβ therapies, which might be modifying this Aβ-astrocyte-tau pathway, showing a higher magnitude of effect in men than women<sup>34</sup>.

The strengths of our study include a large sample size for the main analysis and the use of well-characterized research and population-based cohorts. Limitations include the fact that the analysis using longitudinal tau-PET had a relatively small sample size; thus, replication of this finding is highly desirable. As biomarkers are

naturally continuous, dichotomizing cutoffs are invariably subjected to conceptual and analytical idiosyncrasies and may change depending on the method used. Finally, although our cohort represents significant socioeconomic diversity, the main limitation is that our cohorts are composed mainly of White participants, which limits the generalizability of our findings to a more diverse world population.

In conclusion, our findings suggest that detecting astrocyte reactivity biomarker abnormality is critical to predict whether CU Aβ-positive individuals will develop tau pathology and, consequently, clinical symptoms.

## Online content

Any methods, additional references, Nature Portfolio reporting summaries, source data, extended data, supplementary information, acknowledgements, peer review information; details of author contributions and competing interests; and statements of data and code availability are available at <https://doi.org/10.1038/s41591-023-02380-x>.

## References

- Jack, C. R. Jr et al. Tracking pathophysiological processes in Alzheimer's disease: an updated hypothetical model of dynamic biomarkers. *Lancet Neurol.* **12**, 207–216 (2013).
- Hansson, O. Biomarkers for neurodegenerative diseases. *Nat. Med.* **27**, 954–963 (2021).
- Milà-Alomà, M. et al. Plasma p-tau231 and p-tau217 as state markers of amyloid-β pathology in preclinical Alzheimer's disease. *Nat. Med.* **28**, 1797–1801 (2022).
- Hanseeuw, B. J. et al. Association of amyloid and tau with cognition in preclinical Alzheimer disease: a longitudinal study. *JAMA Neurol.* **76**, 915–924 (2019).

5. Ossenkuppele, R. et al. Accuracy of tau positron emission tomography as a prognostic marker in preclinical and prodromal Alzheimer disease: a head-to-head comparison against amyloid positron emission tomography and magnetic resonance imaging. *JAMA Neurol.* **78**, 961–971 (2021).
6. Ossenkuppele, R. et al. Amyloid and tau PET-positive cognitively unimpaired individuals are at high risk for future cognitive decline. *Nat. Med.* **28**, 2381–2387 (2022).
7. Roberts, R. O. et al. Prevalence and outcomes of amyloid positivity among persons without dementia in a longitudinal, population-based setting. *JAMA Neurol.* **75**, 970–979 (2018).
8. Josephs, K. A., Weigand, S. D. & Whitwell, J. L. Characterizing amyloid-positive individuals with normal tau PET levels after 5 years: an ADNI study. *Neurology* **98**, e2282–e2292 (2022).
9. Nordberg, A. Dementia in 2014. Towards early diagnosis in Alzheimer disease. *Nat. Rev. Neurol.* **11**, 69–70 (2015).
10. Sperling, R. A. et al. Toward defining the preclinical stages of Alzheimer's disease: recommendations from the National Institute on Aging-Alzheimer's Association workgroups on diagnostic guidelines for Alzheimer's disease. *Alzheimers Dement.* **7**, 280–292 (2011).
11. Pike, C. J., Cummings, B. J. & Cotman, C. W. Early association of reactive astrocytes with senile plaques in Alzheimer's disease. *Exp. Neurol.* **132**, 172–179 (1995).
12. Beach, T. G., Walker, R. & McGeer, E. G. Patterns of gliosis in Alzheimer's disease and aging cerebrum. *Glia* **2**, 420–436 (1989).
13. Escartin, C. et al. Reactive astrocyte nomenclature, definitions, and future directions. *Nat. Neurosci.* **24**, 312–325 (2021).
14. Kumar, A., Fontana, I. C. & Nordberg, A. Reactive astrogliosis: a friend or foe in the pathogenesis of Alzheimer's disease. *J. Neurochem.* **164**, 309–324 (2023).
15. Wruck, W. & Adjaye, J. Meta-analysis of human prefrontal cortex reveals activation of GFAP and decline of synaptic transmission in the aging brain. *Acta Neuropathol. Commun.* **8**, 26 (2020).
16. Garwood, C. J., Pooler, A. M., Atherton, J., Hanger, D. P. & Noble, W. Astrocytes are important mediators of A $\beta$ -induced neurotoxicity and tau phosphorylation in primary culture. *Cell Death Dis.* **2**, e167 (2011).
17. Mann, C. N. et al. Astrocytic  $\alpha$ 2-Na<sup>+</sup>/K<sup>+</sup> ATPase inhibition suppresses astrocyte reactivity and reduces neurodegeneration in a tauopathy mouse model. *Sci. Transl. Med.* **14**, eabm4107 (2022).
18. Litvinchuk, A. et al. Complement C3aR inactivation attenuates tau pathology and reverses an immune network deregulated in tauopathy models and Alzheimer's disease. *Neuron* **100**, 1337–1353 (2018).
19. de Calignon, A. et al. Propagation of tau pathology in a model of early Alzheimer's disease. *Neuron* **73**, 685–697 (2012).
20. Wang, P. & Ye, Y. Filamentous recombinant human tau activates primary astrocytes via an integrin receptor complex. *Nat. Commun.* **12**, 95 (2021).
21. Benedet, A. L. et al. Differences between plasma and cerebrospinal fluid glial fibrillary acidic protein levels across the Alzheimer disease continuum. *JAMA Neurol.* **78**, 1471–1483 (2021).
22. Chatterjee, P. et al. Plasma glial fibrillary acidic protein is elevated in cognitively normal older adults at risk of Alzheimer's disease. *Transl. Psychiatry* **11**, 27 (2021).
23. Pereira, J. B. et al. Plasma GFAP is an early marker of amyloid- $\beta$  but not tau pathology in Alzheimer's disease. *Brain* **144**, 3505–3516 (2021).
24. Chatterjee, P. et al. Plasma glial fibrillary acidic protein is associated with 18F-SMBT-1 PET: two putative astrocyte reactivity biomarkers for Alzheimer's disease. *J. Alzheimers Dis.* **92**, 615–628 (2023).
25. Palmqvist, S. et al. Earliest accumulation of  $\beta$ -amyloid occurs within the default-mode network and concurrently affects brain connectivity. *Nat. Commun.* **8**, 1214 (2017).
26. Braak, H. & Braak, E. Neuropathological staging of Alzheimer-related changes. *Acta Neuropathol.* **82**, 239–259 (1991).
27. Jack, C. R. Jr et al. NIA-AA research framework: toward a biological definition of Alzheimer's disease. *Alzheimers Dement.* **14**, 535–562 (2018).
28. Johansson, C. et al. Plasma biomarker profiles in autosomal dominant Alzheimer's disease. *Brain* **146**, 1132–1140 (2023).
29. Verberk, I. M. W. et al. Serum markers glial fibrillary acidic protein and neurofilament light for prognosis and monitoring in cognitively normal older people: a prospective memory clinic-based cohort study. *Lancet Healthy Longev.* **2**, e87–e95 (2021).
30. Shen, X.-N. et al. Plasma glial fibrillary acidic protein in the Alzheimer disease continuum: relationship to other biomarkers, differential diagnosis, and prediction of clinical progression. *Clin. Chem.* **69**, 411–421 (2023).
31. Buckley, R. F. et al. Sex differences in the association of global amyloid and regional tau deposition measured by positron emission tomography in clinically normal older adults. *JAMA Neurol.* **76**, 542–551 (2019).
32. Palta, P. et al. Sex differences in in vivo tau neuropathology in a multiethnic sample of late middle-aged adults. *Neurobiol. Aging* **103**, 109–116 (2021).
33. Tsiknia, A. A. et al. Sex differences in plasma p-tau181 associations with Alzheimer's disease biomarkers, cognitive decline, and clinical progression. *Mol. Psychiatry* **27**, 4314–4322 (2022).
34. van Dyck, C. H. et al. Lecanemab in early Alzheimer's disease. *N. Engl. J. Med.* **388**, 9–21 (2023).

**Publisher's note** Springer Nature remains neutral with regard to jurisdictional claims in published maps and institutional affiliations.

**Open Access** This article is licensed under a Creative Commons Attribution 4.0 International License, which permits use, sharing, adaptation, distribution and reproduction in any medium or format, as long as you give appropriate credit to the original author(s) and the source, provide a link to the Creative Commons license, and indicate if changes were made. The images or other third party material in this article are included in the article's Creative Commons license, unless indicated otherwise in a credit line to the material. If material is not included in the article's Creative Commons license and your intended use is not permitted by statutory regulation or exceeds the permitted use, you will need to obtain permission directly from the copyright holder. To view a copy of this license, visit <http://creativecommons.org/licenses/by/4.0/>.

© The Author(s) 2023

<sup>1</sup>Department of Psychiatry, University of Pittsburgh, Pittsburgh, PA, USA. <sup>2</sup>Graduate Program in Biological Sciences—Biochemistry, Universidade Federal do Rio Grande do Sul, Porto Alegre, Brazil. <sup>3</sup>Department of Psychiatry and Neurochemistry, The Sahlgrenska Academy at the University of Gothenburg, Mölndal, Sweden. <sup>4</sup>Centre for Age-Related Medicine, Stavanger University Hospital, Stavanger, Norway. <sup>5</sup>Department of Old Age Psychiatry, Institute of Psychiatry, Psychology and Neuroscience, King's College London, London, UK. <sup>6</sup>Neuroscience Biomarkers, Janssen Research and Development, La Jolla, CA, USA. <sup>7</sup>Translational Neuroimaging Laboratory, McGill University Research Centre for Studies in Aging, Alzheimer's Disease Research Unit, Douglas Research Institute, Le Centre intégré universitaire de santé et de services sociaux (CIUSSS) de l'Ouest-de-l'Île-de-Montréal; Department of Neurology

and Neurosurgery, Psychiatry and Pharmacology and Therapeutics, McGill University, Montreal, Quebec, Canada. <sup>8</sup>Department of Neurology, School of Medicine, University of Pittsburgh, Pittsburgh, PA, USA. <sup>9</sup>Department of Biostatistics, School of Medicine, University of Pittsburgh, Pittsburgh, PA, USA. <sup>10</sup>Geriatric Research Education and Clinical Center, VA Pittsburgh HS, Pittsburgh, PA, USA. <sup>11</sup>Department of Pharmacology, Universidade Federal do Rio Grande do Sul, Porto Alegre, Brazil. <sup>12</sup>Graduate Program in Biological Sciences: Pharmacology and Therapeutics, Universidade Federal do Rio Grande do Sul, Porto Alegre, Brazil. <sup>13</sup>Brain Institute, PUCRS, Porto Alegre, Brazil. <sup>14</sup>Clinical Neurochemistry Laboratory, Sahlgrenska University Hospital, Mölndal, Sweden. <sup>15</sup>Department of Neurodegenerative Disease, UCL Queen Square Institute of Neurology, London, UK. <sup>16</sup>UK Dementia Research Institute at UCL, London, UK. <sup>17</sup>Hong Kong Center for Neurodegenerative Diseases, Hong Kong, China. <sup>18</sup>Wisconsin Alzheimer's Disease Research Center, University of Wisconsin School of Medicine and Public Health, University of Wisconsin-Madison, Madison, WI, USA. <sup>19</sup>Department of Bioengineering, University of Pittsburgh, Pittsburgh, PA, USA. <sup>20</sup>Department of Psychiatry, University of Illinois, Chicago, IL, USA. <sup>21</sup>Department of Psychology, University of Pittsburgh, Pittsburgh, PA, USA. <sup>22</sup>Department of Epidemiology, University of Pittsburgh School of Public Health, Pittsburgh, PA, USA. <sup>23</sup>Brain Imaging Centre, Montreal Neurological Institute-Hospital, Montreal, Quebec, Canada. ✉e-mail: [pascoalt@upmc.edu](mailto:pascoalt@upmc.edu)

## Methods

### Study population

This study included participants from three centers. The TRIAD cohort (Montreal, Canada, <https://triad.tnl-mcgill.com>) comprised participants with a detailed clinical and cognitive assessment. Exclusion criteria included inability to speak English or French; inadequate visual and auditory capacities for neuropsychological assessment; active substance abuse; major surgery; recent head trauma; medical contraindication for PET or magnetic resonance imaging; currently being enrolled in other studies and neurological, psychiatric or systemic comorbidities that were not adequately treated with a stable medication regimen. CU individuals had a CDR = 0 and no objective cognitive impairment. The study was approved by the Douglas Mental Health University Institute Research Ethics Board and Montreal Neurological Institute PET working committee, and all participants provided written informed consent.

The MYHAT is a population-based study cohort drawn from a Rust Belt region of southwestern Pennsylvania, USA<sup>35</sup>. Participants were selected by age-stratified random sampling from the publicly available voter registration lists over the following two time periods: 2006–2008 and 2016–2019. Inclusion criteria at study entry included the following: (1) 65+ years old, (2) living in a designated town, (3) not residing in long-term care settings, (4) having sufficient hearing and vision to complete neuropsychological testing and (5) having decisional capacity. CU individuals had CDR = 0. All study procedures were approved by the University of Pittsburgh Institutional Review Board, and all participants provided written informed consent.

The Pittsburgh cohort is composed of research volunteers from the following four studies conducted at the University of Pittsburgh: the Heart Strategies Concentrating on Risk Evaluation parent study<sup>36</sup>, the Human Connectome Project<sup>37</sup>, the Normal Aging study<sup>38</sup> and the MsBrain study<sup>39</sup>. All individuals provided written informed consent to one of the above studies. CU individuals were classified using either CDR = 0 or Montreal Cognitive Assessment (MoCA) >25 (for the MsBrain study). Individuals were selected according to cognitive status and plasma biomarker availability. Details of each cohort recruitment are reported in Supplementary Table 6. All study procedures were approved by the University of Pittsburgh Institutional Review Board, and all participants provided written informed consent.

Participants from all cohorts received compensation commensurate with the number of study procedures completed and the duration of participation.

### Plasma and CSF biomarkers

For Pittsburgh and TRIAD cohorts, plasma biomarkers (except for plasma p-tau217) were measured using single-molecule array (Simoa) methods on an HD-X Automated Immunoassay Analyzer (Quanterix), at the Clinical Neurochemistry Laboratory at the University of Gothenburg. Plasma A $\beta$ 42, A $\beta$ 40, GFAP and neurofilament light were quantified with the Neurology 4-Plex E (103670) commercial assays from Quanterix. Plasma p-tau181 (ref. 40) and plasma p-tau231 (ref. 41) were measured using an in-house Simoa assay developed at the University of Gothenburg, as previously described. Plasma p-tau217 (available only for TRIAD) was quantified by scientists at Janssen Research & Development<sup>42</sup>. For the MYHAT cohort, plasma biomarkers were measured using Simoa methods on an HD-X instrument (Quanterix), at the Department of Psychiatry, University of Pittsburgh School of Medicine. Plasma p-tau181 was measured with the p-tau181 V2 Advantage (103714), whereas plasma A $\beta$ 42, A $\beta$ 40, GFAP and neurofilament light concentrations were measured with the Neurology 4-Plex E (103670) commercial assays from Quanterix. For cohorts with no available A $\beta$ -PET (that is, MYHAT and Pittsburgh cohorts), A $\beta$  positivity was determined using plasma A $\beta$ 42/40 based on the expected 30% of A $\beta$  positivity in CU individuals<sup>43</sup>. As younger individuals are more likely to be devoid of AD-related pathology<sup>44,45</sup>, cutoffs for astrocyte reactivity

were generated using the plasma GFAP concentration mean of the 15% youngest A $\beta$ -negative individuals plus 2 s.d. Sensitivity analyses using multiple cutoffs to define A $\beta$  positivity or astrocyte positivity can be found in Supplementary Fig. 2 and Extended Data Table 2. CSF sTREM2 was measured using a Meso-Scale Discovery assay in a subsample in the TRIAD cohort, and the cutoff for positivity was set to correspond to the same percentile of GFAP positivity<sup>46</sup>.

### Magnetic resonance imaging/PET biomarkers

For the TRIAD cohort, A $\beta$ -PET was quantified using the tracer (<sup>18</sup>F)AZD4694 and tau-PET with the tracer (<sup>18</sup>F)MK-6240 in a Siemens high-resolution research tomograph. (<sup>18</sup>F)AZD4694 and (<sup>18</sup>F)MK-6240 images were acquired at 40–70 min and 90–110 min postinjection, respectively. Standardized uptake value ratio (SUVR) was calculated using the whole cerebellum gray matter for (<sup>18</sup>F)AZD4694 and inferior cerebellum gray matter (<sup>18</sup>F)MK-6240 as the reference tissue. Neocortical (<sup>18</sup>F)AZD4694 SUVR value was estimated from a cortical composite, including the precuneus, prefrontal, orbitofrontal, parietal, temporal, anterior and posterior cingulate cortices. Individuals with A $\beta$ -PET neocortical SUVR > 1.55 were considered A $\beta$ -positive<sup>47</sup>. A subsample of 71 CU individuals had a follow-up (<sup>18</sup>F)MK-6240 with a mean of 2.3 years after baseline. Tau-PET Braak stage segmentation has been previously described<sup>48</sup>. Stages consisted of the following regions: Braak I (transentorhinal), Braak II (entorhinal and hippocampus), Braak III (amygdala, parahippocampal gyrus, fusiform gyrus and lingual gyrus), Braak IV (insula, inferior temporal, lateral temporal, posterior cingulate and inferior parietal), Braak V (orbitofrontal, superior temporal, inferior frontal, cuneus, anterior cingulate, supramarginal gyrus, lateral occipital, precuneus, superior parietal, superior frontal and rostromedial frontal) and Braak VI (paracentral, postcentral, precentral and pericalcarine).

A subset of individuals from the MYHAT ( $n = 86$ ) and Pittsburgh ( $n = 64$ ) cohorts had A $\beta$ -PET available for this study. For these individuals, A $\beta$ -PET was quantified using (<sup>11</sup>C)PiB PET acquired at 50–70 min postinjection. A global (<sup>11</sup>C)PiB SUVR index was computed by volume-weighted averaging of all nine composite (<sup>11</sup>C)PiB regions (anterior cingulate, posterior cingulate, insula, superior frontal cortex, orbitofrontal cortex, lateral temporal cortex, parietal, precuneus and ventral striatum). A $\beta$ -PET positivity was defined using a previously established cutoff<sup>49</sup>.

### Statistical analysis

Neuroimaging analyses were carried out using the VoxelStats toolbox version 1 (<https://github.com/sulantha2006/VoxelStats>), a MATLAB-based analytical framework that allows for the execution of multimodal voxel-wise neuroimaging analyses<sup>50</sup> and an R Package for Medical Imaging NetCD (RMINC) v1.5.3.0. Other statistical analyses were performed using the R Statistical Software Package version 3.5.3. Differences between groups in continuous variables (age, cognitive performance (mini-mental state exam (MMSE) or MoCA), biomarkers for A $\beta$ , plasma GFAP, p-tau epitopes and neurofilament light) were assessed using analysis of variance with Tukey correction. Kruskal–Wallis with post hoc Mann–Whitney  $U$  tests were used for categorical or ordinal variables (sex and *APOE*  $\epsilon$ 4 status). For modeling the trajectories of plasma p-tau epitopes as a function of A $\beta$  burden (plasma A $\beta$  or A $\beta$ -PET), we corrected each plasma p-tau epitope value by age and sex. Individuals in the 15th lower percentile for A $\beta$ -PET or the 15th highest percentile for plasma A $\beta$ 42/40 were used as anchors to z-scores. Then, we applied a robust linear regression method (Lowess), using 1,000 robustifying iterations, with a smoother span of 0.95. The effect size of groups (A $\beta^+$ , A $\beta^+$  and A $\beta^+$ /A $\beta^+$ ) in relation to A $\beta^-$ /A $\beta^+$  was estimated using Cohen's  $d$ , in which the dependent variable was the plasma p-tau biomarkers corrected for age and sex (A $\beta^+$  group included individuals positive for astrocyte reactivity but A $\beta^-$ , whereas the A $\beta^+$  group included individuals positive for A $\beta$  but A $\beta^-$ ). The associations between biomarkers



were assessed with linear regressions accounting for age and sex. An interaction term between A $\beta$  burden  $\times$  astrocyte reactivity status/or plasma GFAP as a continuous variable was also added to each model. For analyses including all cohorts, we included cohort as a covariate to adjust for variability in differences between cohorts. For all linear regression analyses,  $z$  scores were centered on the mean within each cohort, and  $z$  scores for plasma A $\beta$  ratio were inverted to pool plasma A $\beta$  and A $\beta$ -PET levels together. To determine sex effects in our findings, we included an interaction term between A $\beta$  burden  $\times$  sex on plasma p-tau considering individuals that are Ast $^-$  and Ast $^+$ . Voxel-wise associations between biomarkers were tested using linear regressions accounting for age and sex, and adjusted for multiple comparisons using a random field theory threshold of  $P < 0.001$  (ref. 51). We evaluated the percentage of abnormality across PET Braak-like stages by dividing the total number of voxels by the number of significant voxels after multiple comparison corrections. We measured the annual rate of progression in ( $^{18}$ F)MK-6240 uptake as the difference between follow-up and baseline uptakes divided by the time between scans.

### Reporting summary

Further information on research design is available in the Nature Portfolio Reporting Summary linked to this article.

### Data availability

All requests for raw and analyzed data and materials can be sent to the corresponding author (T.A.P.) and will be promptly reviewed by the investigators and respective institutions to verify if the request is subject to any intellectual property or confidentiality obligations. Anonymized data will be shared upon request from a qualified academic investigator for the purpose of replicating the procedures and results presented in this article. Any data and materials that can be shared will be released via a material transfer agreement. Data are not publicly available due to information that could compromise the privacy of research participants.

### Code availability

The codes used for the data analyses in our study can be requested from the corresponding author.

### References

35. Ganguli, M. et al. Prevalence of mild cognitive impairment by multiple classifications: the Monongahela-Youghiogheny Healthy Aging Team (MYHAT) project. *Am. J. Geriatr. Psychiatry* **18**, 674–683 (2010).
36. Bambs, C. et al. Low prevalence of “ideal cardiovascular health” in a community-based population: the heart strategies concentrating on risk evaluation (Heart SCORE) study. *Circulation* **123**, 850–857 (2011).
37. Cohen, A. D. et al. Connectomics in brain aging and dementia—the background and design of a study of a connectome related to human disease. *Front. Aging Neurosci.* **13**, 669490 (2021).
38. Aizenstein, H. J. et al. Frequent amyloid deposition without significant cognitive impairment among the elderly. *Arch. Neurol.* **65**, 1509–1517 (2008).
39. Thurston, R. C. et al. Menopausal vasomotor symptoms and white matter hyperintensities in midlife women. *Neurology* **100**, e133–e141 (2023).
40. Karikari, T. K. et al. Blood phosphorylated tau 181 as a biomarker for Alzheimer’s disease: a diagnostic performance and prediction modelling study using data from four prospective cohorts. *Lancet Neurol.* **19**, 422–433 (2020).
41. Ashton, N. J. et al. Plasma p-tau231: a new biomarker for incipient Alzheimer’s disease pathology. *Acta Neuropathol.* **141**, 709–724 (2021).
42. Triana-Baltzer, G. et al. Development and validation of a high-sensitivity assay for measuring p217+tau in plasma. *Alzheimers Dement. (Amst.)* **13**, e12204 (2021).
43. Ossenkoppele, R. et al. Prevalence of amyloid PET positivity in dementia syndromes: a meta-analysis. *JAMA* **313**, 1939–1949 (2015).
44. Jack, C. R. Jr. et al. Defining imaging biomarker cut points for brain aging and Alzheimer’s disease. *Alzheimers Dement.* **13**, 205–216 (2017).
45. Gräsbeck, R. The evolution of the reference value concept. *Clin. Chem. Lab. Med.* **42**, 692–697 (2004).
46. Jensen, C. S. et al. Exercise as a potential modulator of inflammation in patients with Alzheimer’s disease measured in cerebrospinal fluid and plasma. *Exp. Gerontol.* **121**, 91–98 (2019).
47. Theriault, J. et al. Determining amyloid- $\beta$  positivity using (18)F-AZD4694 PET imaging. *J. Nucl. Med.* **62**, 247–252 (2021).
48. Pascoal, T. A. et al. 18F-MK-6240 PET for early and late detection of neurofibrillary tangles. *Brain* **143**, 2818–2830 (2020).
49. Cohen, A. D. et al. Classification of amyloid-positivity in controls: comparison of visual read and quantitative approaches. *Neuroimage* **71**, 207–215 (2013).
50. Mathotaarachchi, S. et al. VoxelStats: a MATLAB package for multi-modal voxel-wise brain image analysis. *Front. Neuroinform.* **10**, 20 (2016).
51. Worsley, K. J., Taylor, J. E., Tomaiuolo, F. & Lerch, J. Unified univariate and multivariate random field theory. *Neuroimage* **23**, S189–S195 (2004).

### Acknowledgements

We thank all TRIAD, MYHAT and Pittsburgh studies personnel for their effort and participants for their time, data and specimens. We would like to thank the following funding agencies that supported this work: NIH, National Institute of Aging (grants R01AG075336 and R01AG073267 to T.A.P.; RF1AG053504 and R01AG053504 to R.C.T.; RF1AG053504 to P.M.; R01AG052528, P01AG14449 and P01AG025204 to M.D.I.); NIH, National Heart Lung and Blood Institute (grants R01HL105647 and K24HL123565 to R.C.T.); Alzheimer’s Association (grants AARFD-22-974627 to B.B.; AACSF-20-648075 to T.A.P.; AARF-21-850325 to T.K.K.; AARFD-22-923814 to P.C.L.F.; AARGD-21-850670 to E.R.Z.; ADSF-21-831376-C, ADSF-21-831381-C and ADSF-21-831377-C to H.Z.); CAPES (grant 88887.336490/2019-00 to B.B.); CNPq (grant 200691/2021-0 to J.P.F.-S); Fonds de Recherche du Québec—Santé (FRQS; Chercheur Boursier, grant 2020-VICO-279314 to P.R.-N.); CIHR-CCNA Canadian Consortium of Neurodegeneration in Aging (grants MOP-11-51-31; RFN 152985, 159815, 162303 to P.R.-N.); Weston Brain Institute (grants 8400707, 8401154 and 8401103 to P.R.-N.); Colin Adair Charitable Foundation (grant to P.R.-N.); Swedish Research Council, Vetenskapsrådet (grant 2021-03244 to T.K.K.); Wallenberg Scholar (grant 2022-01018 to H.Z.; 2017-00915 and 2022-00732 to K.B.); BrightFocus Foundation (grant A2020812F to T.K.K.); Swedish Alzheimer Foundation (Alzheimerfonden; grant AF-930627 to T.K.K.; AF-930351, AF-939721 and AF-968270 to K.B.); Swedish Brain Foundation (Hjärnfonden; grant FO2020-0240 to T.K.K.); Agneta Prytz-Folkes & Gösta Folkes Foundation (grant 2020-00124 to T.K.K.); European Union’s Horizon Europe research and innovation program (grant 101053962 to H.Z.); Swedish State Support for Clinical Research (grant ALFGBG-71320 to H.Z.); Alzheimer Drug Discovery Foundation (ADDF; grant 201809-2016862 to H.Z.); Bluefield Project, the Olav Thon Foundation, the Erling-Persson Family Foundation, Stiftelsen för Gamla Tjänarinnor, Hjärnfonden, Sweden (grant FO2022-0270 to H.Z.); European Union’s Horizon 2020 research and innovation program under the Marie Skłodowska-Curie (grant 860197 (MIRIAD) to H.Z.); the European Union Joint Program—Neurodegenerative Disease Research (grant JPN2021-00694 to H.Z. and JPN2019-466-236 to K.B.); The UK Dementia Research Institute at UCL (grant

UKDRI-1003 to H.Z.); National Academy of Neuropsychology (grant ALZ-NAN-22-928381 to E.R.Z.); Fundação de Amparo a pesquisa do Rio Grande do Sul (FAPERGS; grant 21/2551-0000673-0 to E.R.Z.); Instituto Serrapilheira (grant Serra-1912-31365 to E.R.Z.); Hjärfonden (grants FO2017-0243 and ALZ2022-0006 to K.B.); The Swedish state under the agreement between the Swedish government and the County Councils, the ALF agreement (grants ALFGBG-715986 and ALFGBG-965240 to K.B.); The Alzheimer's Association 2021 Zenith Award (grant ZEN-21-848495 to K.B.) and NIH, National Institute of Aging (grants AG052521 and R37 AG023651 supported the MYHAT cohort). Studies composing the Pittsburgh cohort were financed by NIH, National Institute of Aging (grants P30 AG066468, P01AG025204, RF1AG025516, RF1AG052525, R01AG052446 and R01AG052446).

### Author contributions

B.B. and T.A.P. designed the study. T.A.P., P.R.-N., M.G., H.J.A., W.E.K., B.E.S., P.M., R.C.T., O.L.L., A.D.C., S.G., C.T., J.T., S.S., J.S., N.R., F.Z.L. and A.L.B. were responsible for participants recruitment, cohort procedures and sample collection. B.B., P.C.L.F., T.K.K., H.Z., K.B., N.J.A., A.L.B., G.T.-B. and H.C.K. acquired blood biomarker data. T.A.P., P.R.-N., B.E.S., C.T., J.T., S.S., J.S., N.R., F.Z.L. and A.L.B. acquired imaging data. B.B., T.A.P., G.P., J.P.F.-S., D.T.L. and D.L.T. contributed to data analyses, interpretation and designing of figures. B.B., and T.A.P. wrote the initial draft of the paper. G.P., P.C.L.F., J.P.F.-S., D.T.L., T.K.K., A.L.B., N.J.A., P.R.-N., W.E.K., R.C.T., C.T., J.T., S.S., F.Z.L., H.Z., K.B., G.T.-B., V.L.V., M.D.I., E.R.Z. and D.L.T. edited and revised the paper for intellectual content.

### Competing interests

H.C.K. and G.T.-B. are employees and stockholders of Johnson & Johnson. H.Z. has served on scientific advisory boards and/or as a consultant for Abbvie, Acumen, Alector, Alzinova, ALZPath, Annexon, Apellis, Artery Therapeutics, AZTherapies, CogRx, Denali, Eisai, Nervgen, Novo Nordisk, Optoceutics, Passage Bio, Pinteon Therapeutics, Prothena, Red Abbey Labs, reMYND, Roche, Samumed, Siemens Healthineers, Triplet Therapeutics and Wave; has given lectures in symposia sponsored by Cellectricon, Fujirebio, Alzecure, Biogen and Roche and is a cofounder of Brain Biomarker Solutions in Gothenburg AB (BBS), which is a part of the GU Ventures Incubator

Program (outside submitted work). K.B. has served as a consultant, at advisory boards, or at data monitoring committees for Abcam, Axon, Biogen, JOMDD/Shimadzu, Julius Clinical, Lilly, MagQu, Novartis, Prothena, Roche Diagnostics and Siemens Healthineers and is a cofounder of Brain Biomarker Solutions in Gothenburg AB (BBS), which is a part of the GU Ventures Incubator Program, all unrelated to the work presented in this paper. S.G. has served as a scientific advisor to Cerveau Therapeutics. E.R.Z. serves on the scientific advisory board of Next Innovative Therapeutics (Nintx). P.R.-N. has served on scientific advisory boards and/or as a consultant for Eisai, Novo Nordisk and Roche. N.J.A. has given lectures in symposia sponsored by Lilly and Quanterix. M.D.I. has received research funding from GE Healthcare and Avid Radiopharmaceuticals. R.C.T. serves as a consultant, advisor and/or on the medical advisory board of Happify Health, Astellas Pharma, Bayer and Hello Therapeutics. GE Healthcare holds a license agreement with the University of Pittsburgh based on the PiB PET technology described in this paper. W.E.K. is a co-inventor of PiB and, as such, has a financial interest in this license agreement. GE Healthcare provided no grant support for this study and had no role in the design or interpretation of results or preparation of this paper. The other authors declare no competing interests.

### Additional information

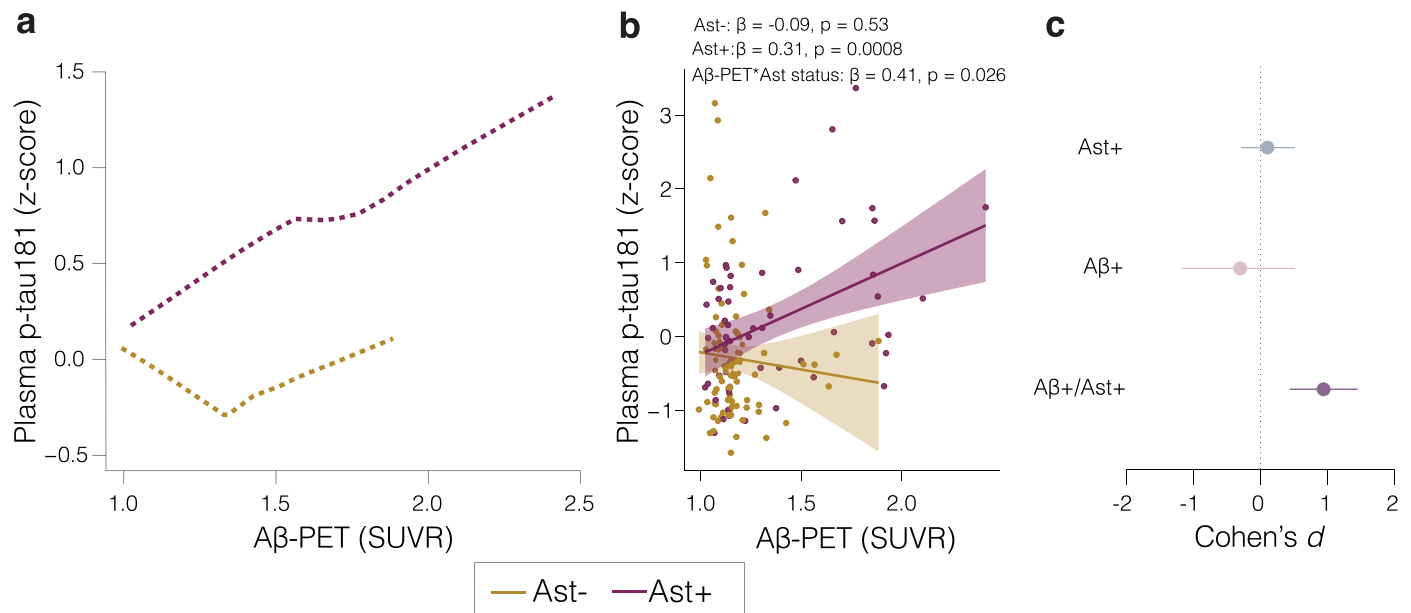
**Extended data** is available for this paper at <https://doi.org/10.1038/s41591-023-02380-x>.

**Supplementary information** The online version contains supplementary material available at <https://doi.org/10.1038/s41591-023-02380-x>.

**Correspondence and requests for materials** should be addressed to Tharick A. Pascoal.

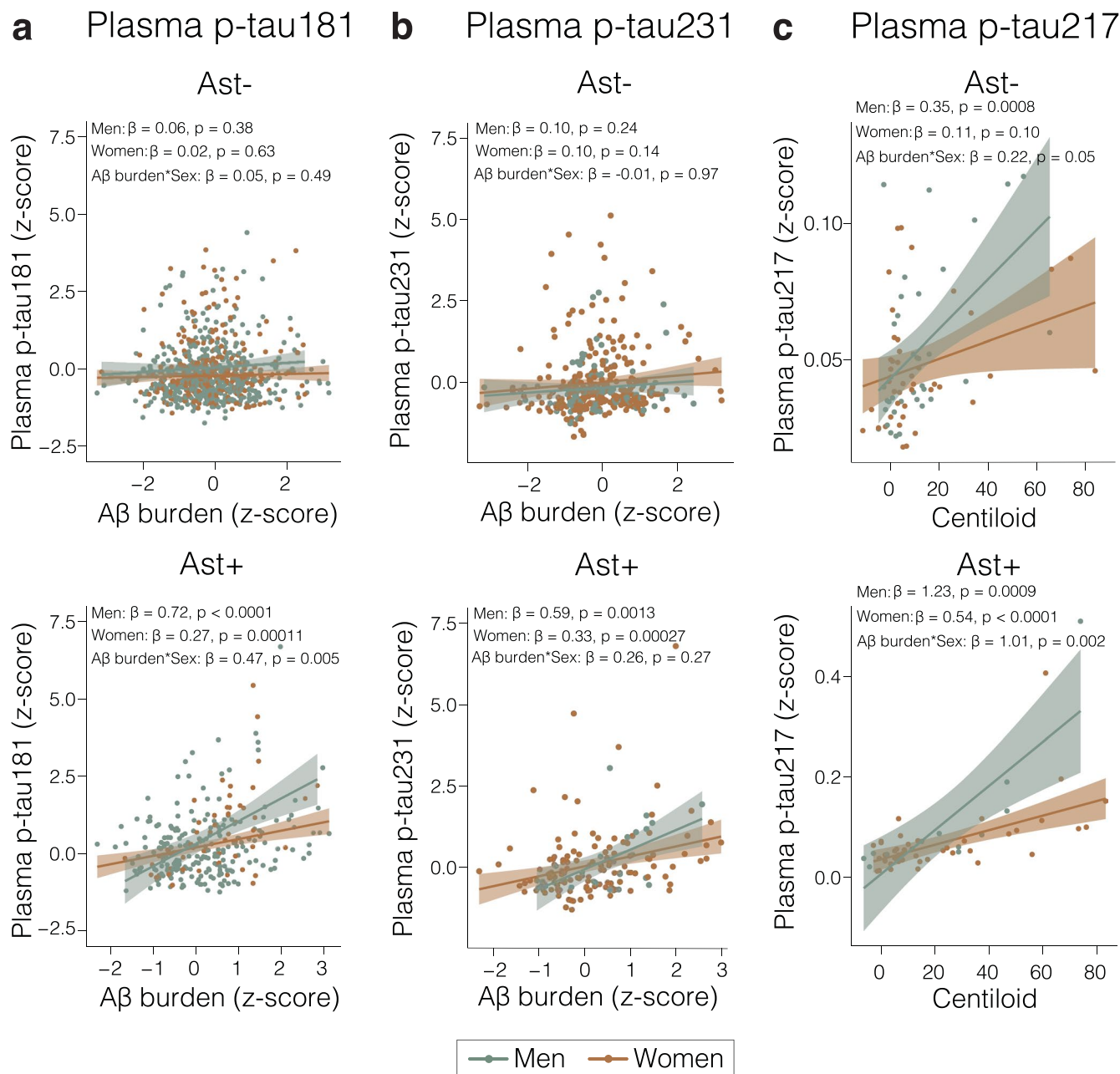
**Peer review information** *Nature Medicine* thanks Reisa Sperling, Wai Haung Yu and Matthias Brendel for their contribution to the peer review of this work. Primary Handling Editor: Jerome Staal, in collaboration with the *Nature Medicine* team.

**Reprints and permissions information** is available at [www.nature.com/reprints](http://www.nature.com/reprints).



**Extended Data Fig. 1 | Impact of astrocyte reactivity in the association between Aβ-PET and plasma p-tau181 in a subset of individuals from MYHAT and Pittsburgh cohorts.** **a**, Robust locally weighted regressions show that plasma p-tau181 increases as a function of Aβ-PET only in Ast+ ( $n = 150$ ). **b**, Linear regressions revealed an interaction between Aβ-PET and astrocyte reactivity status on p-tau181 levels ( $n = 150$ ). The plots show regression line with their

respective 95% confidence intervals. P-values were computed using linear regression models adjusted by age and sex. In addition, the Aβ-PET  $\times$  astrocyte reactivity status interaction was also computed. Red lines and dots represent Ast+ and orange lines and dots represent Ast- individuals. **c**, Cohen's  $d$  analysis accounting for age and sex shows the effect sizes of Aβ and Ast on plasma p-tau181 ( $n = 150$ ). The error bars denote the 95% confidence intervals.



**Extended Data Fig. 2 | The impact of astrocyte reactivity on the A $\beta$  and tau association is greater in men.** Linear regressions showing the effect of sex on the associations of A $\beta$  with (a) plasma p-tau181, (b) plasma p-tau231 and (c) plasma p-tau217 in individuals negative (Ast-, top) and positive (Ast+, bottom)

for astrocyte reactivity. The plots show regression line with their respective 95% confidence intervals and the p-values were adjusted by age and sex. In addition, a plasma A $\beta$  burden  $\times$  sex interaction was also computed. Orange lines and dots represent women and green lines and dots represent men.

Extended Data Table 1 | Associations between plasma p-tau181 and A $\beta$  burden according to astrocyte reactivity status

Study population	$\beta$ (95% CI)	T-value (df)	p-value
<i>Model: Plasma p-tau181 ~ A<math>\beta</math> burden * Astrocyte reactivity status + covariates</i>			
<b>All cohorts</b>			
Ast-	0.04 (-0.03 – 0.10)	1.06 (737)	0.29
Ast+	0.34 (0.22 – 0.46)	5.37 (267)	<0.0001
<i>A<math>\beta</math> burden * Ast status</i>	0.31 (0.18 – 0.44)	4.62 (1008)	<0.0001
<b>Pittsburgh cohort</b>			
Ast-	0.05 (-0.08 – 0.16)	0.82 (257)	0.41
Ast+	0.35 (0.13 – 0.57)	3.10 (90)	0.003
<i>A<math>\beta</math> burden * Ast status</i>	0.29 (0.04 – 0.53)	2.30 (349)	0.022
<b>MYHAT cohort</b>			
Ast-	0.01 (-0.09 – 0.09)	0.06 (393)	0.95
Ast+	0.20 (0.03 – 0.37)	2.26 (113)	0.026
<i>A<math>\beta</math> burden * Ast status</i>	0.19 (0.01 – 0.38)	2.07 (508)	0.039
<b>TRIAD cohort</b>			
Ast-	0.12 (-0.05 – 0.29)	1.39 (81)	0.17
Ast+	0.57 (0.31 – 0.83)	4.36 (58)	<0.0001
<i>A<math>\beta</math> burden * Ast status</i>	0.46 (0.15 – 0.77)	2.92 (141)	0.004

Abbreviations: Ast-: reactive astrocyte negative; Ast+: reactive astrocyte positive; p-tau: phosphorylated tau. We inverted the values for plasma A $\beta$  ratio in the analysis to pool plasma A $\beta$  and A $\beta$ -PET levels together. Covariates: age, sex, and cohort (when all studies were evaluated together). P-values were computed using linear regression models adjusted by age, sex, and cohort (when appropriate) for individuals classified as Ast- and Ast+. In addition, the A $\beta$  burden  $\times$  astrocyte reactivity status interaction was also computed.

**Extended Data Table 2 | Sensitivity analyses using multiple plasma GFAP cutoffs to determine astrocyte positivity**

GFAP cutoff defined as mean + s.d from controls ( <i>n</i> = number of Ast+ individuals)	$\beta$ 3 interaction (95% CI)	T-value (df)	p-value
<i>Model: Plasma p-tau181 ~ A<math>\beta</math> burden*Astrocyte reactivity status + covariates</i>			
0.5 s.d ( <i>n</i> =599)	0.15 (0.02 – 0.27)	2.36 (1008)	0.019
1.0 s.d ( <i>n</i> =474)	0.18 (0.06 – 0.30)	2.99 (1008)	0.003
1.5 s.d ( <i>n</i> =360)	0.23 (0.10 – 0.35)	3.64 (1008)	0.0003
2.0 s.d ( <i>n</i> =273)	0.31 (0.18 – 0.44)	4.62 (1008)	<0.0001
2.5 s.d ( <i>n</i> =211)	0.27 (0.13 – 0.41)	3.73 (1008)	0.0002
3.0 s.d ( <i>n</i> =174)	0.26 (0.11 – 0.41)	3.42 (1008)	0.0006
<i>Model: Plasma p-tau231 ~ A<math>\beta</math> burden*Astrocyte reactivity status + covariates</i>			
0.5 s.d ( <i>n</i> =325)	0.13 (-0.05 – 0.31)	1.39 (495)	0.165
1.0 s.d ( <i>n</i> =264)	0.16 (-0.01 – 0.34)	1.82 (495)	0.069
1.5 s.d ( <i>n</i> =200)	0.20 (0.03 – 0.38)	2.32 (495)	0.021
2.0 s.d ( <i>n</i> =156)	0.26 (0.08 – 0.45)	2.84 (495)	0.004
2.5 s.d ( <i>n</i> =125)	0.25 (0.06 – 0.44)	2.54 (495)	0.011
3.0 s.d ( <i>n</i> =105)	0.23 (0.04 – 0.44)	2.32 (495)	0.021
<i>Model: Plasma p-tau217 ~ A<math>\beta</math> burden*Astrocyte reactivity status + covariates</i>			
0.5 s.d ( <i>n</i> =106)	0.22 (-0.19 – 0.64)	1.08 (130)	0.281
1.0 s.d ( <i>n</i> =90)	0.24 (-0.15 – 0.64)	1.20 (130)	0.232
1.5 s.d ( <i>n</i> =72)	0.38 (0.07 – 0.70)	2.43 (130)	0.016
2.0 s.d ( <i>n</i> =62)	0.53 (0.25 – 0.81)	3.74 (130)	0.0003
2.5 s.d ( <i>n</i> =50)	0.51 (0.24 – 0.80)	3.65 (130)	0.0004
3.0 s.d ( <i>n</i> =45)	0.54 (0.26 – 0.82)	3.88 (130)	0.0002

Abbreviations: Ast<sup>-</sup>: reactive astrocyte negative; Ast<sup>+</sup>: reactive astrocyte positive; GFAP: glial fibrillary acidic protein; s.d.: standard deviation; p-tau: phosphorylated tau. The highest  $\beta$ -estimate was obtained using GFAP cutoff calculated as the mean + 2.0s.d. of controls devoid of A $\beta$  pathology for all plasma p-tau epitopes. Covariates: age, sex, and cohort. We inverted the values for plasma A $\beta$  ratio in the analysis to pool plasma A $\beta$  and A $\beta$ -PET levels together. P-values were computed using linear regression models adjusted by age, sex and cohort (when appropriate) for individuals classified as Ast<sup>-</sup> and Ast<sup>+</sup>. In addition, the A $\beta$  burden  $\times$  astrocyte reactivity status interaction was also computed.

Extended Data Table 3 | Sensitivity analysis adjusting for APOE $\epsilon$ 4 status

Study population	$\beta$ (95% CI)	T-value (df)	p-value
<i>Model: Plasma p-tau181 ~ A<math>\beta</math> burden*Astrocyte reactivity status + age + sex + APOE <math>\epsilon</math>4 status</i>			
A $\beta$ burden*Ast status	0.35 (0.20 – 0.49)	4.70 (762)	<0.0001
<i>Model: Plasma p-tau181 ~ A<math>\beta</math> burden + age + sex + APOE <math>\epsilon</math>4 status</i>			
(Within Ast- and Ast+ groups)			
<b>Ast-</b>			
A $\beta$ burden	0.01 (-0.07 – 0.09)	0.27 (551)	0.79
APOE $\epsilon$ 4 status	0.05 (-0.13 – 0.22)	0.51 (551)	0.61
<b>Ast+</b>			
A $\beta$ burden	0.37 (0.23 – 0.51)	5.20 (206)	<0.0001
APOE $\epsilon$ 4 status	0.06 (0.13 – 0.57)	0.37 (206)	0.71
<i>Model: Plasma p-tau231 ~ A<math>\beta</math> burden*Astrocyte reactivity status + age + sex + APOE <math>\epsilon</math>4 status</i>			
A $\beta$ burden*Ast status	0.26 (0.05 – 0.48)	2.38 (260)	0.018
<i>Model: Plasma p-tau231 ~ A<math>\beta</math> burden + age + sex + APOE <math>\epsilon</math>4 status</i>			
(Within Ast- and Ast+ groups)			
<b>Ast-</b>			
A $\beta$ burden	0.15 (0.02 – 0.28)	2.23 (165)	0.027
APOE $\epsilon$ 4 status	0.24 (-0.02 – 0.50)	1.84 (165)	0.068
<b>Ast+</b>			
A $\beta$ burden	0.45 (0.26 – 0.64)	4.76 (91)	<0.0001
APOE $\epsilon$ 4 status	-0.01 (-0.52 – 0.51)	-0.03 (91)	0.979
<i>Model: Plasma p-tau217 ~ A<math>\beta</math> burden*Astrocyte reactivity status + age + sex + APOE <math>\epsilon</math>4 status</i>			
A $\beta$ burden*Ast status	0.54 (0.26 – 0.83)	3.83 (129)	0.0002
<i>Model: Plasma p-tau217 ~ A<math>\beta</math> burden + age + sex + APOE <math>\epsilon</math>4 status</i>			
(Within Ast- and Ast+ groups)			
<b>Ast-</b>			
A $\beta$ burden	0.21 (0.09 – 0.32)	3.69 (73)	0.0004
APOE $\epsilon$ 4 status	-0.002 (-0.22 – 0.21)	-0.02 (73)	0.983
<b>Ast+</b>			
A $\beta$ burden	0.76 (0.51 – 1.01)	6.02 (53)	<0.0001
APOE $\epsilon$ 4 status	-0.53 (-1.22 – 0.17)	-1.52 (53)	0.134

Abbreviations: Ast-: reactive astrocyte negative; Ast+: reactive astrocyte positive; p-tau: phosphorylated tau. We inverted the values for plasma A $\beta$  ratio in the analysis to pool plasma A $\beta$  and A $\beta$ -PET levels together. P-values were computed using linear regression models adjusted by age, sex and cohort (when appropriate) for individuals classified as Ast- and Ast+. In addition, the A $\beta$  burden  $\times$  astrocyte reactivity status interaction was also computed.

**Extended Data Table 4 | Associations between plasma p-tau231 and p-tau217 and A $\beta$  burden according to astrocyte reactivity status**

Study population	$\beta$ (95% CI)	T-value (df)	p-value
<i>Model: Plasma p-tau231 ~ A<math>\beta</math> burden*Astrocyte reactivity status + covariates</i>			
<i>All cohorts</i>			
Ast-	0.10 (-0.005 – 0.20)	1.87 (341)	0.062
Ast+	0.36 (0.21 – 0.52)	4.62 (151)	<0.0001
<i>A<math>\beta</math> burden*Ast status</i>	0.26 (0.08 – 0.45)	2.84 (495)	0.004
<i>A<math>\beta</math> burden*Ast continuous</i>	0.10 (-0.008 – 0.15)	1.77 (495)	0.078
<i>Model: Plasma p-tau217 ~ A<math>\beta</math> burden*Astrocyte reactivity status + covariates</i>			
Ast-	0.21 (0.10 – 0.28)	3.74 (74)	0.0004
Ast+	0.76 (0.50 – 1.01)	5.91 (54)	<0.0001
<i>A<math>\beta</math> burden*Ast status</i>	0.53 (0.25 – 0.81)	3.74 (130)	0.0003
<i>A<math>\beta</math> burden*Ast continuous</i>	0.18 (0.05 – 0.31)	2.76 (130)	0.007

Abbreviations: Ast-: reactive astrocyte negative; Ast+: reactive astrocyte positive; p-tau: phosphorylated tau. Covariates: age, sex, and cohort. We inverted the values for plasma A $\beta$  ratio in the analysis to pool plasma A $\beta$  and A $\beta$ -PET levels together. P-values were computed using linear regression models adjusted by age, sex and cohort (when appropriate) for individuals classified as Ast- and Ast+. In addition, the A $\beta$  burden  $\times$  astrocyte reactivity status interaction was also computed.



**Extended Data Table 5 | Associations between plasma p-tau and A $\beta$  burden according to microglial activation (MA) status in the TRIAD cohort**

Study population	$\beta$ (95% CI)	T-value (df)	p-value
<i>Model: Plasma p-tau ~ A<math>\beta</math> burden*Microglial activation + covariates</i>			
<i>Plasma p-tau181 (n=67)</i>			
MA-	0.25 (0.01 – 0.50)	2.08 (35)	0.045
MA+	0.14 (-0.39 – 0.32)	0.66 (24)	0.52
<i>A<math>\beta</math> burden*MA continuous</i>	0.07 (-0.68 – 0.83)	0.19 (61)	0.85
<i>A<math>\beta</math> burden*MA dichotomized</i>	-0.10 (-0.43 – 0.22)	-0.64 (61)	0.53
<i>Plasma p-tau231 (n=67)</i>			
MA-	0.49 (0.31 – 0.66)	5.69 (35)	<0.0001
MA+	0.69 (0.07 – 1.30)	2.31 (24)	0.03
<i>A<math>\beta</math> burden*MA continuous</i>	0.07 (-0.19 – 0.34)	0.55 (61)	0.58
<i>A<math>\beta</math> burden*MA dichotomized</i>	0.16 (-0.44 – 0.77)	0.54 (61)	0.59
<i>Plasma p-tau217 (n=65)</i>			
MA-	0.59 (0.26 – 0.93)	3.6 (34)	0.001
MA+	0.10 (-0.21 – 0.40)	0.63 (22)	0.54
<i>A<math>\beta</math> burden*MA continuous</i>	0.10 (-0.31 – 0.51)	0.48 (58)	0.63
<i>A<math>\beta</math> burden*MA dichotomized</i>	-0.26 (-1.20 – 0.69)	-0.55 (58)	0.59

Abbreviations: MA-: microglial activation negative; MA+: microglial activation positive; p-tau: phosphorylated tau. Covariates: age and sex. The effect of astrocyte reactivity in this subpopulation remained significant (A $\beta$  burden\*Astrocyte positivity status:  $\beta$ =0.50, 95% CI=0.15–0.85; t-value=2.87; p-value=0.006). P-values were computed using linear regression models adjusted by age, sex and cohort (when appropriate) for individuals classified as MA- and MA+. In addition, the A $\beta$  burden\*microglial activation status interaction was also computed.

## Reporting Summary

Nature Portfolio wishes to improve the reproducibility of the work that we publish. This form provides structure for consistency and transparency in reporting. For further information on Nature Portfolio policies, see our [Editorial Policies](#) and the [Editorial Policy Checklist](#).

### Statistics

For all statistical analyses, confirm that the following items are present in the figure legend, table legend, main text, or Methods section.

n/a Confirmed

- The exact sample size ( $n$ ) for each experimental group/condition, given as a discrete number and unit of measurement
- A statement on whether measurements were taken from distinct samples or whether the same sample was measured repeatedly
- The statistical test(s) used AND whether they are one- or two-sided  
*Only common tests should be described solely by name; describe more complex techniques in the Methods section.*
- A description of all covariates tested
- A description of any assumptions or corrections, such as tests of normality and adjustment for multiple comparisons
- A full description of the statistical parameters including central tendency (e.g. means) or other basic estimates (e.g. regression coefficient) AND variation (e.g. standard deviation) or associated estimates of uncertainty (e.g. confidence intervals)
- For null hypothesis testing, the test statistic (e.g.  $F$ ,  $t$ ,  $r$ ) with confidence intervals, effect sizes, degrees of freedom and  $P$  value noted  
*Give  $P$  values as exact values whenever suitable.*
- For Bayesian analysis, information on the choice of priors and Markov chain Monte Carlo settings
- For hierarchical and complex designs, identification of the appropriate level for tests and full reporting of outcomes
- Estimates of effect sizes (e.g. Cohen's  $d$ , Pearson's  $r$ ), indicating how they were calculated

*Our web collection on [statistics for biologists](#) contains articles on many of the points above.*

### Software and code

Policy information about [availability of computer code](#)

Data collection

Data analysis

For manuscripts utilizing custom algorithms or software that are central to the research but not yet described in published literature, software must be made available to editors and reviewers. We strongly encourage code deposition in a community repository (e.g. GitHub). See the Nature Portfolio [guidelines for submitting code & software](#) for further information.

### Data

Policy information about [availability of data](#)

All manuscripts must include a [data availability statement](#). This statement should provide the following information, where applicable:

- Accession codes, unique identifiers, or web links for publicly available datasets
- A description of any restrictions on data availability
- For clinical datasets or third party data, please ensure that the statement adheres to our [policy](#)

All requests for raw and analyzed data and materials can be sent to the corresponding author (TAP) and will be promptly reviewed by the investigators and respective institutions to verify if the request is subject to any intellectual property or confidentiality obligations. Anonymized data will be shared upon request from

## Human research participants

Policy information about [studies involving human research participants and Sex and Gender in Research](#).

### Reporting on sex and gender

The findings presented here were observed in both men and women. However, a stronger effect of astrocyte reactivity on the association between amyloid and tau was observed in men. Sex, not gender, was used in the study design based on self-report. There is no information about disaggregated sex and gender for these individuals. Sex was added as a covariate in all models. Sex-effects were also tested in the associations between amyloid and tau.

### Population characteristics

Supplemental Tables 1,2,3 and 5. Briefly, the main study population is composed by 1,016 cognitively unimpaired individuals from two research and one population-based cohort. The mean age of this population is 69.6 (std 8.9) years-old, 69.4% were women.

### Recruitment

The Translational Biomarkers in Aging and Dementia (TRIAD) cohort (Montreal, Canada, <https://triad.tnl-mcgill.com>) comprised participants with a detailed clinical and cognitive assessment. Exclusion criteria included inability to speak English or French, inadequate visual and auditory capacities for neuropsychological assessment, active substance abuse, major surgery, recent head trauma, medical contraindication for positron emission tomography (PET) or magnetic resonance imaging (MRI), currently being enrolled in other studies, and neurological, psychiatric, or systemic comorbidities that were not adequately treated with a stable medication regimen. The Monongahela-Youghiogheny Healthy Aging Team (MYHAT) is a population-based study cohort drawn from a Rust Belt region of southwestern Pennsylvania, USA. Participants were selected by age-stratified random sampling from the publicly available voter registration lists over two time periods: 2006-2008 and 2016-2019. Inclusion criteria at study entry included: 1) 65+ years old, 2) living in a designated town, 3) not residing in long-term care settings, 4) having sufficient hearing and vision to complete neuropsychological testing, and 5) having decisional capacity. The Pittsburgh cohort is composed of research volunteers from four studies conducted at the University of Pittsburgh: the Heart Strategies Concentrating on Risk Evaluation (Heart SCORE) parent study, the Human Connectome Project (HCP), the Normal Aging study, and the MsBrain. While our cohort represents significant socioeconomic diversity, the it is mainly composed of White participants.

### Ethics oversight

For TRIAD, the study was approved by the Douglas Mental Health University Institute Research Ethics Board and Montreal Neurological Institute PET working committee and all participants provided written informed consent. For MYHAT and Pittsburgh cohorts all procedures were approved by the University of Pittsburgh Institutional Review Board and all participants provided written informed consent. Participants from all cohorts received compensation commensurate with the amount of study procedures completed and duration of participation.

Note that full information on the approval of the study protocol must also be provided in the manuscript.

## Field-specific reporting

Please select the one below that is the best fit for your research. If you are not sure, read the appropriate sections before making your selection.

Life sciences  Behavioural & social sciences  Ecological, evolutionary & environmental sciences

For a reference copy of the document with all sections, see [nature.com/documents/nr-reporting-summary-flat.pdf](https://nature.com/documents/nr-reporting-summary-flat.pdf)

## Life sciences study design

All studies must disclose on these points even when the disclosure is negative.

### Sample size

The sample size here was determined based on the number of participants with available plasma GFAP, plasma p-tau and amyloid-B (plasma or PET), from three prospective studies (MYHAT [n=514], Pittsburgh [n = 355] and TRIAD [n=147]). All participants with baseline plasma GFAP, plasma p-tau and amyloid-B data available were analyzed in this study.

### Data exclusions

Individuals with no plasma GFAP, plasma p-tau and plasma or PET amyloid data were excluded from the analysis. All cognitively impaired individuals (CDR > 0 or MoCA < 25) were excluded. Young individuals (age < 25) were also excluded from the TRIAD cohort. For plasma amyloid data, outliers were removed interquartile range intervals.

### Replication

Our results were replicated in three independent cohorts.

### Randomization

In these cohort studies (observational studies) no allocation into experimental groups were performed, therefore randomization is not relevant to this study. Statistical analyses were controlled for potential confounding effect of age and sex.

### Blinding

All biomarker (PET and plasma) collection and analyses performed in this study were performed blinded to clinical diagnosis.

# Reporting for specific materials, systems and methods

We require information from authors about some types of materials, experimental systems and methods used in many studies. Here, indicate whether each material, system or method listed is relevant to your study. If you are not sure if a list item applies to your research, read the appropriate section before selecting a response.

## Materials & experimental systems

- | n/a                                 | Included in the study                                  |
|-------------------------------------|--|
| <input checked="" type="checkbox"/> | <input type="checkbox"/> Antibodies                    |
| <input checked="" type="checkbox"/> | <input type="checkbox"/> Eukaryotic cell lines         |
| <input checked="" type="checkbox"/> | <input type="checkbox"/> Palaeontology and archaeology |
| <input checked="" type="checkbox"/> | <input type="checkbox"/> Animals and other organisms   |
| <input checked="" type="checkbox"/> | <input type="checkbox"/> Clinical data                 |
| <input checked="" type="checkbox"/> | <input type="checkbox"/> Dual use research of concern  |

## Methods

- | n/a                                 | Included in the study                           |
|-------------------------------------|---|
| <input checked="" type="checkbox"/> | <input type="checkbox"/> ChIP-seq               |
| <input checked="" type="checkbox"/> | <input type="checkbox"/> Flow cytometry         |
| <input checked="" type="checkbox"/> | <input type="checkbox"/> MRI-based neuroimaging |